Journal of Alloys and Compounds 500 (2010) 227–230

Contents lists available at ScienceDirect

Journal of Alloys and Compounds

journal homepage: www.elsevier.com/locate/jallcom

# Thermoelectric performance of textured $Ca_{3-x}Yb_xCo_4O_{9-\delta}$ ceramics

Jie Xu, Changping Wei*, Kun Jia

*College of Material Science and Engineering, Changchun University of Science and Technology, No.7989, Weixing Road, Changchun 130022, People's Republic of China*

ARTICLE INFO

*Article history:*
Received 16 November 2009
Received in revised form 29 March 2010
Accepted 1 April 2010
Available online 9 April 2010

*Keywords:*
Ceramics
Sol–gel processes
Thermoelectric

ABSTRACT

A series of ceramics $Ca_{3-x}Yb_xCo_4O_{9-\delta}$ ($x = 0$, 0.2, 0.3, 0.4, 0.5) were prepared by the sol–gel method followed by pressing and sintering. The thermoelectric properties were characterized from room temperature to 870 K. Partial $Yb^{3+}$ ions substituting for $Ca^{2+}$ sites enter into the lattices without any impurity phase, and form highly textured structure. $Ca_{3-x}Yb_xCo_4O_{9-\delta}$ samples exhibit semiconducting behavior and the Seebeck coefficient increase strikingly by increasing the content of $Yb^{3+}$ ion. The thermal conductivity varies within narrow limits, and the figure of merit ZT of $Ca_{2.8}Yb_{0.2}Co_4O_{9-\delta}$ exceeds 0.16 at 870 K.



## 1. Introduction

Thermoelectric materials can interconvert thermal power and electric energy, thus may play significant role in the efficient utilization of energy sources [1]. Thermoelectric oxides, as a representative class of thermoelectric materials, have attracted increasing attention due to their outstanding advantages such as highly thermal and chemical stability and low toxicity compared to the intermetallic alloys. Recently, many kinds of thermoelectric oxides with highly thermoelectric performance have been reported, including $NaCo_2O_4$, $Ca_3Co_4O_{9-\delta}$, $Ca_2Co_2O_5$, $Bi_2Sr_2Co_2O_y$, $TiSr_2Co_2O_y$, $SrTiO_3$, $CaMnO_3$, and so on [2–6]. Among them, the calcium cobalt oxide $Ca_3Co_4O_{9-\delta}$ is regarded as one of the promising candidates for thermoelectric application. It is well known that $Ca_3Co_4O_{9-\delta}$ is a misfit-layered compound built up from two monoclinic sublattices, the rock-salt layer [$Ca_2CoO_3$] and $CdI_2$-type layer [$CoO_2$] subsystems, exhibiting an incommensurate periodicity along the *b*-axis [7]. And the highly thermoelectric performance of $Ca_3Co_4O_{9-\delta}$ is due to its layered structure.

Recently, different approaches have been developed in order to further enhance the thermoelectric performance of $Ca_3Co_4O_{9-\delta}$. For instances, by combining special post-treatment method, such as spark plasma sintering, sinter-forging, hot pressing, magnetic field and thermo-forging methods, the properties of $Ca_3Co_4O_{9-\delta}$ could be improved though adjusting the dense and textured state of polycrystalline oxide [8–10]. In addition, because of the special lamellar structure of $Ca_3Co_4O_{9-\delta}$, the carrier concentration and mobility are important factors on electrical properties. Therefore, partial substitution is also an effective way to enhance properties of $Ca_3Co_4O_{9-\delta}$ by optimizing the carrier density. Nong et al. reported that the thermoelectric properties of $Ca_3Co_4O_{9-\delta}$ could be enhanced by partial $Ga^{3+}$ substitution for Co site [11]. And other reports revealed that by substituting Ca site with $Bi^{2+}$, $Na^+$, $Ag^+$, $Ba^{2+}$ ions can also improve the thermoelectric performance of $Ca_3Co_4O_{9-\delta}$ [12–14].

In this paper, we chose the rare earth ion $Yb^{3+}$ to doping into $Ca_3Co_4O_{9-\delta}$, partial substituting Ca site, because the 4f energy level of the rare earth element approaches to the Fermi level [15]. Textured thermoelectric ceramics $Ca_{3-x}Yb_xCo_4O_{9-\delta}$ have been prepared by the citrate sol–gel method followed by pressing and sintering. The phase composition and microstructure have been discussed and the effect of substitution on thermoelectric properties has been investigated. The results show that partial $Yb^{3+}$ substitution for $Ca^{2+}$ site can improve the thermoelectric power effectively.

## 2. Experimental

The $Ca_{3-x}Yb_xCo_4O_{9-\delta}$ ($x = 0$, 0.2, 0.3, 0.4, 0.5) ceramics were prepared by citrate complexation sol–gel method followed by pressing and sintering. $Yb(NO_3)_3$ (prepared by dissolving 99.99% $Yb_2O_3$ in nitric acid and evaporating the solvent), $Ca(NO_3)_2{\cdot}4H_2O$, $Co(NO_3)_2{\cdot}6H_2O$ and $C_6H_8O_7{\cdot}H_2O$ in the appropriate stoichiometric ratio were mixed and dissolved in distilled water. The solution was heated to 340 K for 1 h when the constituents reacted to form the purple and transparent sol. The sol was dried at 400 K to form the gel. The dry gel was calcined in the air at 1073 K for 3 h to obtain $Ca_{3-x}Yb_xCo_4O_{9-\delta}$ powder. The powder was grinded and pressed into square tablet 3 mm × 20 mm × 20 mm under the pressure of 30 MPa, then the tablet was sintered in the air at 1123 K for 8 h.

For the microstructure analyses, emission scanning electron microscopy (ESEM) coupled with an energy dispersive X-ray spectroscopy (EDAX) was used. X-ray diffraction (XRD) patterns were recorded on a Rigaku D/max-rA X-ray diffractometer with Cu Kα1 radiation (λ = 0.15405 nm) operated at 40 kV, 20 mV current at room temperature. Infrared spectra (IR) were investigated using a Nicolet

* Corresponding author. Tel.: +86 431 85350155.
*E-mail addresses:* jiexu0121@hotmail.com (J. Xu), changpingwei@yahoo.com.cn (C. Wei).

0925-8388/$ – see front matter © 2010 Elsevier B.V. All rights reserved.
doi:10.1016/j.jallcom.2010.04.014

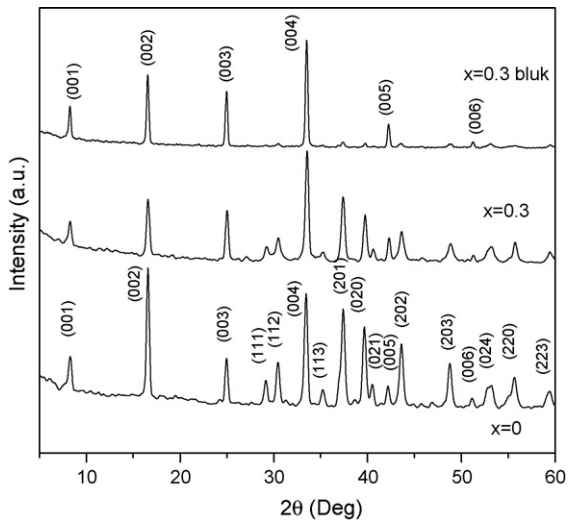


**Fig. 1.** XRD spectra of $Ca_{3-x}Yb_xCo_4O_{9-\delta}$ powders ($x = 0$, 0.3) and ceramic bulk ($x = 0.3$).

DXFT-IR spectrometer over a range of 400–4000 $cm^{-1}$ using the KBr pressed disc method. TG–DTA study was applied in flowing air at temperature range 300–1200 K (Shimadzu DTA-60). Electrical resistivity ($\rho$) and Seebeck coefficients ($S$) were measured simultaneously using a ZEM-1 apparatus in the temperature range of 300–870 K. The thermal conductivity ($\kappa$) in the temperature range from 300 to 870 K was calculated using the value of the density of the specimen measured by Archimedes' principle, and the thermal diffusivity and specific heat measured by a laser flash method (Shinkuriko:TC-7000).

## 3. Results and discussion

The XRD spectra of $Ca_{3-x}Yb_xCo_4O_{9-\delta}$ powders ($x = 0$, 0.3) and $Ca_{3-x}Yb_xCo_4O_{9-\delta}$ ceramic bulk ($x = 0.3$) are shown in Fig. 1, which are identical to the standard JCPSD card (21-0139), indicating the formation of single-phase compounds, and $Yb^{3+}$ ions doping into the lattices without changing the lattice structure. X-ray diffraction of $Ca_{3-x}Yb_xCo_4O_{9-\delta}$ ceramic bulk ($x = 0.3$) reveals strong peaks indexed as (0 0 $l$), which implies that the crystal grains align along the $c$-axis to form highly textured structure [16]. In addition, XRD analysis indicated that when the content of $Yb^{3+}$ ion reached to $x = 0.5$, the diffraction pattern showed an impurity peak (not shown here), confirming that the suitable range of doping should be among $x = 0$–0.4. The lattice parameters of the samples were calculated based on the X-ray diffraction data and shown in Table 1. It can be found that the lattice parameters $b$ and $c$ of $Ca_{2.7}Yb_{0.3}Co_4O_{9-\delta}$ powder decrease somewhat simultaneously, and the unit-cell volume decrease slightly compared with $Ca_3Co_4O_{9-\delta}$, which should be due to the ionic radius of $Yb^{3+}$ (0.99 Å) is very close to that of $Ca^{2+}$ (1.00 Å). The reduction of the unit-cell volume of $Ca_{2.7}Yb_{0.3}Co_4O_{9-\delta}$ ceramic compared with $Ca_{2.7}Yb_{0.3}Co_4O_{9-\delta}$ powder sample can be interpreted that the pressure leads to the cell orientation. Table 2 gives the EDAX analysis results of $Ca_{3-x}Yb_xCo_4O_{9-\delta}$ ($x = 0$–0.4) samples. The composition of the samples can be found that the content of Co is unvaried, and the content of Ca is slightly decrease with increasing the content of $Yb^{3+}$ ion, that indicating $Yb^{3+}$ partial substituting $Ca^{2+}$ site in the lattice.

**Table 1**
Lattice parameter $a$, $b$, $c$, $\beta$ and unit-cell volume $v$ of samples.

| Sample | $a$ (nm) | $b$ (nm) | $c$ (nm) | $\beta$ (°) | $v$ (nm$^3$) |
|---|---|---|---|---|---|
| $Ca_3Co_4O_{9-\delta}$ powder | 0.4837 | 0.4559 | 1.0843 | 98.17 | 0.2367 |
| $Ca_{2.7}Yb_{0.3}Co_4O_{9-\delta}$ powder | 0.4837 | 0.4553 | 1.0817 | 98.24 | 0.2358 |
| $Ca_{2.7}Yb_{0.3}Co_4O_{9-\delta}$ ceramics | 0.4837 | 0.4542 | 1.0795 | 98.25 | 0.2348 |

**Table 2**
EDAX results showing the cation ratio of the samples.

| Samples | Co | Ca | Yb |
|---|---|---|---|
| $Ca_3Co_4O_{9-\delta}$ | 4 | 3 | 0 |
| $Ca_{2.8}Yb_{0.2}Co_4O_{9-\delta}$ | 4 | 2.81 | 0.16 |
| $Ca_{2.7}Yb_{0.3}Co_4O_{9-\delta}$ | 4 | 2.67 | 0.31 |
| $Ca_{2.6}Yb_{0.4}Co_4O_{9-\delta}$ | 4 | 2.62 | 0.35 |

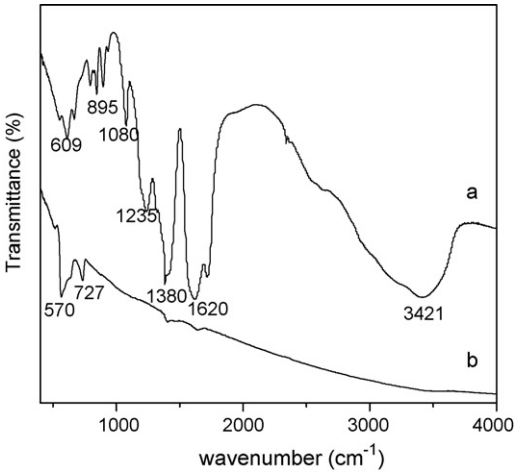


**Fig. 2.** IR spectra of (a) gel and (b) $Ca_{2.7}Yb_{0.3}Co_4O_{9-\delta}$ powder.

Fig. 2 shows the IR spectra of the dry gel and powder of $Ca_{2.7}Yb_{0.3}Co_4O_{9-\delta}$ sample. During the formation of the gel, citric acid ($H_3Cit$) dissociates to the citric acid radical $Cit^{3-}$, which complexes with the metal nitrates to give citrates. The characteristic absorption peaks of the gel are shown in Table 3. The spectrum of $Ca_{2.7}Yb_{0.3}Co_4O_{9-\delta}$ powder shows without absorption peaks for any organic groups. The bands centered at 727 and 570 $cm^{-1}$ can be assigned to the Ca–O bond (or Yb–O) and the Co–O bond, respectively, indicating that the organic matters have been completely decomposed, giving a pure compound $Ca_{2.7}Yb_{0.3}Co_4O_{9-\delta}$.

The TG–DTA curves of the dry gel of $Ca_{2.7}Yb_{0.3}Co_4O_{9-\delta}$ sample (Fig. 3) show an exothermic peak at 440 K, which is accompanied by a weight loss that was assigned to the evaporation of adsorbing water and the decomposition of nitric acid. The strong exothermic peak observed between 560 and 730 K accompanied by drastic weight loss due to the vigorous combustion of nitrates and citrates. The exothermic peak at 750 K was assigned to the decomposition of the residual citric acid. Above 780 K, the weight loss was assigned to the oxidation reaction and crystal formation. Because all the reactions were overlapping, the TG curve shows a continuous weight loss process [17]. According to the DTA analysis, the formation process of $Ca_{3-x}Yb_xCo_4O_{9-\delta}$ can be described as the removal of organic phase by calcination to give CaO, $Yb_2O_3$ and CoO, then the oxidation of CoO to $Co_3O_4$ by heating in the air, finally the reaction of inorganic oxides. In addition, it should be pointed out that the sintering temperature of the $Ca_{3-x}Yb_xCo_4O_{9-\delta}$ ceramics should be controlled among the temperature range 1023–1123 K. Above 1193 K,

**Table 3**
IR absorption bands of the gel.

| Absorption band ($cm^{-1}$) | Assignation |
|---|---|
| 3421 | $\nu$OH stretching vibration |
| 1620, 1720 | C=O stretching vibration |
| 1380 | $\nu$CO + $\delta$OH (in plane) |
| 1080, 1235 | C–O stretching vibration |
| 895 | $\delta$OH (out plane) |
| 609 | C–O–M stretching vibration |

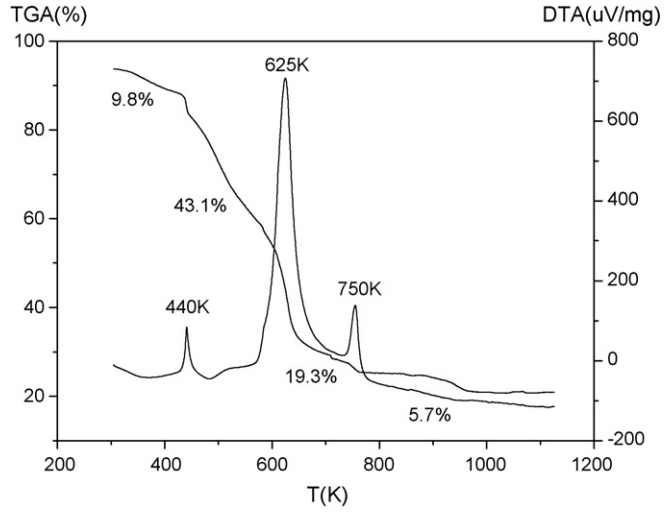


**Fig. 3.** TG–DTA curves of the gel of $Ca_{2.7}Yb_{0.3}Co_4O_{9-\delta}$.

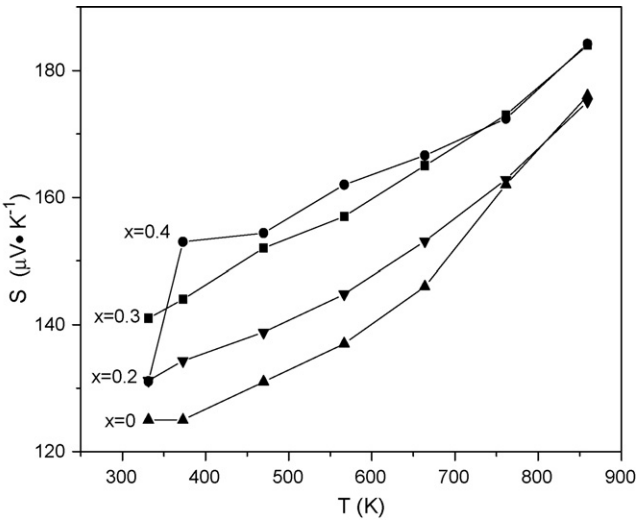


**Fig. 5.** Temperature dependence of the thermoelectric power.

$Ca_{3-x}Yb_x$ $Co_4O_{9-\delta}$ will decompose to $Ca_{3-x}Yb_xCo_2O_6$, whose electrical resistivity is much higher than that of $Ca_{3-x}Yb_xCo_4O_{9-\delta}$.

The thermoelectric properties of materials are usually characterized by the dimensionless figure of merit ($ZT = S^2T/\rho\kappa$). Good thermoelectric material should have large thermoelectric power (Seebeck coefficient $S$), and small electrical resistivity $\rho$ and thermal conductivity $\kappa$. However, these three parameters are all functions of the carrier concentration and dependent on each other. Therefore, we should optimize the carrier concentration to enhance the ZT value.

Fig. 4 shows the temperature dependence of electrical resistivity of $Ca_{3-x}Yb_xCo_4O_{9-\delta}$ samples. It can be found that the resistivity of $Ca_3Co_4O_{9-\delta}$ increases with increasing temperature, showing metallic-like behavior, while the resistivity of $Ca_{3-x}Yb_xCo_4O_{9-\delta}$ samples decrease with increasing temperature, showing semiconductor-like behavior; and the trend becomes obviously with increasing the $Yb^{3+}$ content. This phenomenon can be interpreted by the fact that ionized impurity scattering predominate the major carriers, resulting in increasing carrier mobility. The electrical resistivity depends on the carrier concentration and mobility, which relate to the impurity content and temperature [18]. We can see from Fig. 4 that the resistivity of $Ca_3Co_4O_{9-\delta}$ is lower than that of the doped samples, which seems to be caused by the doping decreases the carrier concentration. However, with increasing temperature, the difference of resistivity between the doped and undoped samples decreases, and when the temperature exceeds 773 K, the resistivity of $Ca_{2.8}Yb_{0.2}Co_4O_{9-\delta}$ is lower than that of the undoped $Ca_3Co_4O_{9-\delta}$. This result can be interpreted that when the $Yb^{3+}$ ions enter the forbidden region of $Ca_3Co_4O_{9-\delta}$ to form an impurity donor level. At low temperature, there may be a transition of the electrons from the donor level to the valence band, followed by recombination with positive holes, inducing the decrease of the carrier density and the increase of resistivity. As the temperature rise, the electrons in the donor level obtain the enough energy to make transition to the conduction band, reducing the probability of transition to the valence band and resulting in the increase of the holes concentration. As the temperature increases further, it is also possible for electrons in the valence band obtain the enough energy to make a transition to the conduction band, so the carrier concentration increases further. In this way, the resistivity of $Ca_{2.8}Yb_{0.2}Co_4O_{9-\delta}$ gradually approaches that of the undoped sample.

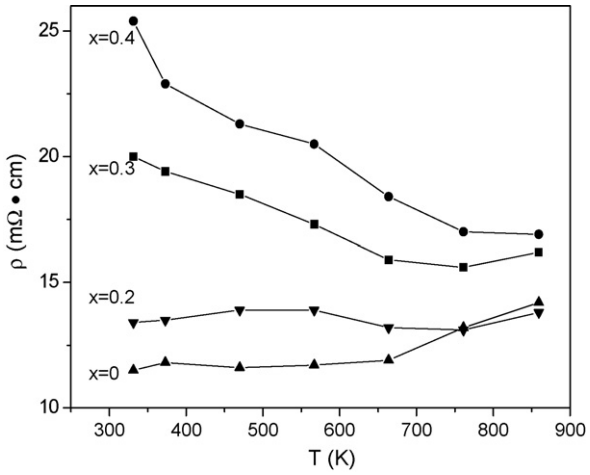


**Fig. 4.** Temperature dependence of the electrical resistivity.

Fig. 5 shows the temperature dependence of Seebeck coefficient of $Ca_{3-x}Yb_xCo_4O_{9-\delta}$ samples. All the samples show positive-type Seebeck coefficient over the entire temperature range, indicating p-type semiconductors and positive holes conduction dominating the transport properties. The thermoelectric conversion procedure can be interpreted as follows. When the temperature is different between two sides of the material, the carrier concentration adjacent to the low temperature side is lower than that adjacent to the high temperature side. Therefore, the carriers (positive holes) diffuse from the hot side to the cold side and accumulate at the cold side, forming an electric field oriented from the cold side to the hot side. In the electric field, positive holes drift along the direction of the electric field. When the diffusion and drift of the positive holes reach an equilibrium state, the electric potential difference establishes between the two sides of the material. In this way, the carriers convert thermal power into electric energy. From the figure, the Seebeck coefficient increases with increasing $Yb^{3+}$ content, with the maximum value of 184 μV/K at 870 K for $Ca_{2.7}Yb_{0.3}Co_4O_{9-\delta}$. As already reported, the electronic configuration of the Yb atom is $4f^{14}6\,s^2$, and the electronic configuration of $Yb^{3+}$ ion is $4f^{13}$. According to the formula, as the 4f energy level of $Yb^{3+}$ is close to the Fermi level, $Yb^{3+}$-doping increases the density of state $N_v$, at the same time the hole concentration $p$ is reduced (as explained above), therefore, the Seebeck coefficient of the doped samples

**Table 4**
Power factors for $Ca_{3-x}Yb_xCo_4O_{9-\delta}$ at 770 K and 870 K.

| Doping content | $P$ (μW/mK$^2$)770 K | $P$ (μW/mK$^2$)870 K |
|---|---|---|
| $x=0$ | 198 | 217 |
| $x=0.2$ | 201 | 222 |
| $x=0.3$ | 190 | 209 |
| $x=0.4$ | 174 | 200 |

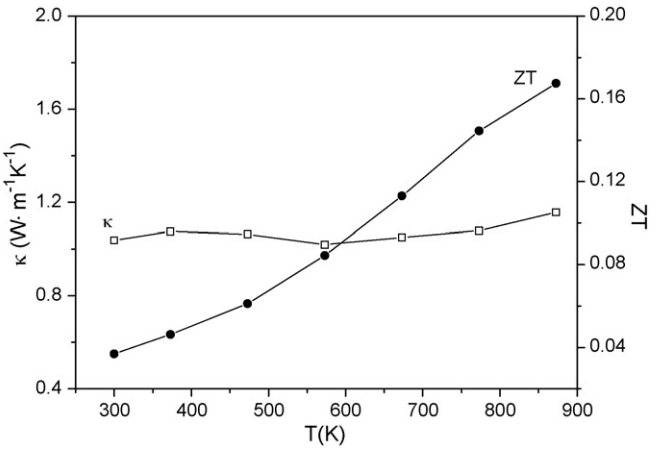


**Fig. 6.** Temperature dependence of the thermal conductivity and ZT for $Ca_{2.8}Yb_{0.2}Co_4O_{9-\delta}$.

increases [19].

$$S = \frac{k_B}{e}\left(\frac{3}{2} - \ln\frac{p}{N_v}\right)$$

In the formula, $p$ is the hole concentration, $N_v$ is the density of states of the valence band, $k_B$ is the Boltzmann constant, $T$ is the temperature in Kelvin and $e$ is the electronic charge.

The power factors ($P = S^2/\rho$) for $Ca_{3-x}Yb_xCo_4O_{9-\delta}$ samples at 770 and 870 K are listed in Table 4. By comparison, the maximum value is 222 μW/mK$^2$ for $Ca_{2.8}Yb_{0.2}Co_4O_{9-\delta}$ at 870 K, due to its lowest resistivity and relatively higher Seebeck coefficient.

For $Ca_{2.8}Yb_{0.2}Co_4O_{9-\delta}$, the thermal conductivity $\kappa$ was calculated, and the temperature dependences of ZT values are shown in Fig. 6. The thermal conductivity $\kappa$ can be represented by the sum of carrier component ($\kappa_C$) and phonon component ($\kappa_P$) as $\kappa = \kappa_C + \kappa_P$. The carrier component $\kappa_C$ can be calculated using the Wiedemann–Franz law $\kappa_C = LT/\rho$, where $L = 2.4 \times 10^{-8}$ V$^2$/K$^2$ is the Lorenz number, $\rho$ the electrical resistivity and $T$ is Kelvin temperature. The phonon component $\kappa_P$ was calculated from the equation $\kappa = D \times C_p \times d$, where $d = 3.6$ g/cm$^3$ is the density of the specimen of $Ca_{2.8}Yb_{0.2}Co_4O_{9-\delta}$, $D$ is the thermal diffusivity, and $C_p$ is the specific heat. The calculations indicated that $\kappa$ varied within narrow limits around 1.0 W/mK from room temperature to 870 K, which suggested that doping influenced little on the thermal conductivity, and that the phonon component $\kappa_P$ was the dominant factor in the total thermal conductivity, exceeding 90%. The figure of merit ZT value increases with increasing temperature significantly, and ZT value reaches 0.16 at 870 K for $Ca_{2.8}Yb_{0.2}Co_4O_{9-\delta}$.

## 4. Conclusions

In summary, highly textured $Ca_{3-x}Yb_xCo_4O_{9-\delta}$ ($x = 0$, 0.2, 0.3, 0.4) ceramics have been synthesized. Partial $Yb^{3+}$substituting for $Ca^{2+}$ site leads to significant increase of the Seebeck coefficient. The difference of resistivity between the doped and undoped samples decreases with the temperature increasing. The thermal conductivity varies within narrow limits around 1.0 W/mK from room temperature to 870 K, and the ZT value is 0.16 at 870 K for $Ca_{2.8}Yb_{0.2}Co_4O_{9-\delta}$. These results suggest that $Ca_{3-x}Yb_xCo_4O_{9-\delta}$ ceramics may be potential thermoelectric material for practical application.

## Acknowledgment

This work was supported by the “Home Program”: Help Our Motherland through Elite Intellectual Resources from Overseas of China Association for Science and Technology (No. 08068).

## References

[1] M. Ito, D. Furumoto, Scripta Mater. 55 (2006) 533–536.
[2] E. Guilmeau, M. Pollet, D. Grebille, M. Hervieu, H. Muguerra, R. Cloots, M. Mikami, R. Funahashi, Inorg. Chem. 46 (2007) 2124–2131.
[3] D. Kenfaui, D. Chateigner, M. Gomina, J.G. Noude, J. Alloys Compd. 490 (2010) 472–479.
[4] P.S. Liu, G. Chen, J. Pei, Y. Cui, D.Q. Lu, N. Zhou, H.Z. Xian, Physica B 403 (2008) 808–1812.
[5] S. Ohta, T. Nomura, H. Ohta, M. Hirano, H. Hosono, K. Koumoto, Appl. Phys. Lett. 87 (2005) 092108.
[6] F. Kawashima, X.Y. Huang, K. Hayashi, Y. Miyazaki, T. Kajitani, J. Electron. Mater. 38 (2009) 1159–1162.
[7] A.C. Masset, C. Michel, A. Maignan, M. Hervieu, O. Toulemonde, F. Studer, B. Raveau, Phys. Rev. B 62 (2000) 166–175.
[8] J.G. Noudem, M. Prevel, A. Veres, D. Chateigner, J. Galy, J. Electroceram. 22 (2009) 91–97.
[9] H. Fukutomi, Y. Konno, K. Okayasu, M. Hasegawa, H. Nakatsugawa, Mater. Sci. Eng. A 527 (2009) 61–64.
[10] M. Prevel, S. Lemonnier, Y. Klein, S. Hébert, D. Chateigner, J. Appl. Phys. 98 (2005) 093706.
[11] N.V. Nong, C.J. Liu, M. Ohtaki, J. Alloys Compd. 491 (2010) 53–56.
[12] F.P. Zhang, Q.M. Lu, J.X. Zhang, J. Alloys Compd. 484 (2009) 550–554.
[13] Y. Wang, Y. Sui, J. Cheng, X. Wang, W. Su, J. Alloys Compd. 477 (2009) 817–821.
[14] Y. Masuda, D. Nagahama, H. Itahara, T. Tani, W.S. Seo, K. Koumoto, J. Mater. Chem. 13 (2003) 1094–1099.
[15] D. Flahaut, T. Mihara, R. Funahashi, N. Nabeshima, K. Lee, H. Ohta, K. Koumoto, J. Appl. Phys. 100 (2006) 084911.
[16] H. Fukutomi, E. Iguchi, Acta Mater. 55 (2007) 4213–4219.
[17] M.S. Lizer, P. Smaczynski, K. Koziowska, E.B. Grzesik, J. Plewa, H. Altenburg, J. Eur. Ceram. Soc. 25 (2005) 1997–2001.
[18] P. Limelette, S. Hébert, V. Hardy, R. Fresard, C. Simon, A. Maignan, Phys. Rev. Lett. 97 (2006) 046601.
[19] M. Shizuya, M. Isobe, Y. Baba, T. Nakuro, M. Osada, K. Kosuda, S. Takenouchi, Y. Matsui, E.T. Muromachi, J.Solid State Chem. 180 (2007) 249–259.